Journal Name

Dynamic Article Links ▶

Cite this: DOI: 10.1039/c0xx00000x

www.rsc.org/xxxxxx

ARTICLE TYPE

YStokes Emission in GdF_3:Nd^{3+} Nanoparticles for Bioimaging Probe

M. Pokhrel,[a] L.C. Mimun[a], B. Yust[a], G.A. Kumar[a] A. Dhanale[b], L. Tang[b] and D.K. Sardar[a]*

Department of Physics and Astronomy, University of Texas at San Antonio, San Antonio, Texas 78249

[b]Department of Biomedical Engineering University of Texas at San Antonio One UTSA Circle, San Antonio, Texas 78249

Received (in XXX, XXX) Xth XXXXXXXXX 20XX, Accepted Xth XXXXXXXXX 20XX
DOI: 10.1039/b000000x

ESI-S1. Quantum Yield (QY) Setup

For the quantum yield (QY) measurements in powder form, a barium sulfate coated (203 mm in diameter) integrating sphere from Oriel (Model 70451) was used with a mounted spectrofluorometer sample chamber on the side, opposite to the excitation source. Powder sample was held in a specially designed sample holder with a quartz window to hold the powder in place and mounted at the sample port of the integrating sphere. The diffuse fluorescence spectra from the nanoparticles and the laser profile were recorded with the spectrofluorometer exciting the sample with an 808 nm continuous power tunable fiber coupled Fabry Perot laser diode (Thorlab, Model LM14S2). Different excitation power densities were achieved by changing the current at diode controller. Three different power densities were used to evaluate the QY for Nd^{3+} doped GdF_3 nanoparticles. The fluorescence output from the sphere was collected via a liquid light guide (LLG) with a specially designed baffle that prevents the direct entry of the exciting laser beam into the detector. The LLG collects the light from the sphere and fed to the InGAS detector through the emission monochromator.

The QY was measured finding the ratio of the area under the corrected emission spectra as shown in Fig. S1(a) to the difference in corrected area under the diffuse reflectance of the excitation spectra for the sample and the reference as shown in inset of Fig. S1(b). The spectra were collected after diffuse reflectance from the sample relative to a non-absorbing standard (barium sulfate) at the excitation

wavelength and emission spectra under the same condition as shown in Fig. S1 (c). The emission (860-1450 nm) and excitation spectra (800-830 nm) not absorbed by the sample and reference was measured using the Quanta Master 51 spectrofluorimeter from Photon Technology International Inc. (PTI) with a InGAS_detector as shown in Fig S1(a).

Including all the possible error like reflectivity of the reference (<5%), particle size effects (< 5 %), diffuse reflectance from the front part of the quartz window of the sample holder (< 5 %); we estimate the error in calculated QYs is about 15 %. Similarly, we estimate the error for power density calculation is about 15 %. Furthermore, relative measurement method has been used to check the accuracy of our QY measurement setup with integrating sphere using the known infrared efficiency of a dye (IR-140).

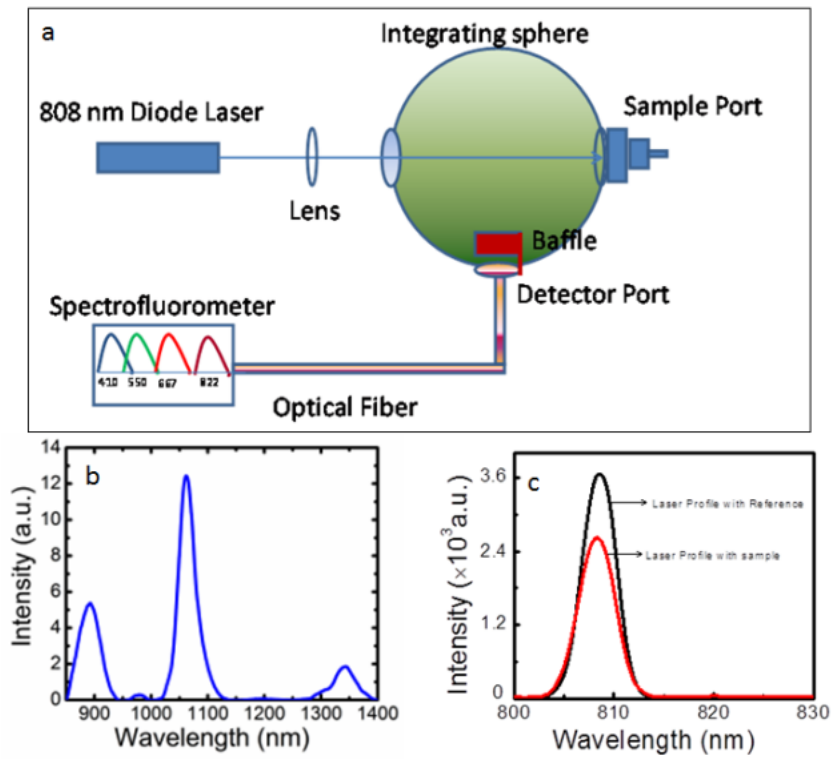

Fig. S1. (a) Integrating sphere setup for downconversion (Stokes emission) and upconversion QY measurement, (b) Stokes emission spectrum for GdF_3: 1% Nd^{3+} cantered at 875, 1064, and 1350 nm at the excitation power density of 4.77 ± 2 W/cm^2 under 808 nm excitation, (c) Laser profile under the ref (black) and sample (red) for, GdF_3: 1% Nd^{3+}

ESI-S2 Defects in the Nanocrystals

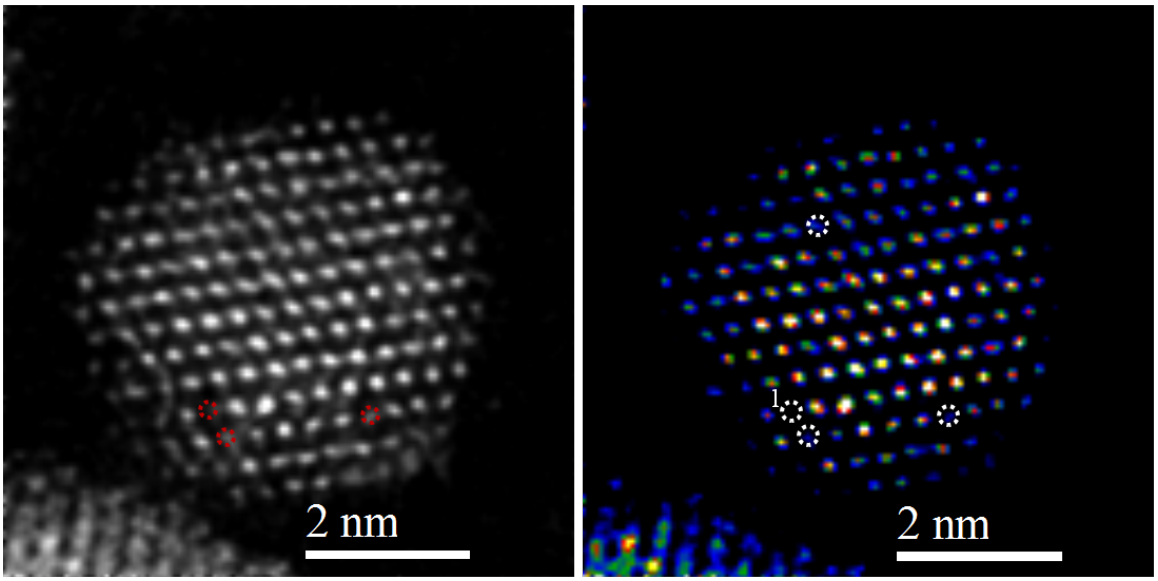

Fig. S2 Z-contrast High Angular Annular Dark Field (HAADF) image of GdF_3: 2% Nd^{3+} nanoparticles. The higher intensity region corresponds to the Gd-rich atomic columns while lower intensity region corresponds to the F-rich atomic columns. The intensity of atomic columns shows that even in some cases the atoms on the surface are missing and also presents some voids in the structure. The voids are represented by white circle 1 in the figure at right frame.

ESI-S3 Quantum Yield (QY) Calibration

We have been reporting the luminescence efficiency of upconversion particles with minimum error using photo multiplier tube (PMT) for the visible emissions under 980 nm excitation.[1, 2] Similarly, there have been many publications reporting the QY for visible emissions under UV excitations. In both cases, PMT actually gives the actual photon counts, which makes luminescence efficiency measurement easier. However, there are no literatures reporting the NIR to IR QY in rare earth (RE) doped system either using integrating sphere or by relative method. Moreover, downconversion (Stokes emission) QY measurement setup in NIR region is different from the reported upconversion quantum yield measurement setup and uses the InGaS detector. But, due to the lack of standard reporting NIR to NIR absolute quantum yield, we confirm our NIR QY setup measuring the 1550 nm downconversion efficiency for different concentrations of Er/Yb doped in La_2O_2S at 2.4 ±0.36 W/cm^2

under 980 nm excitation. The efficiency obtained for 1550 nm for a range of Yb/Er concentrations are shown in Fig. S3. We can see that at low Yb/Er ratio of 0.1 (Yb=1 mol%, Er = 9 mol%) efficiency reaches a highest value of near 21 ± 3.15 %, Yb/Er ratio of 1 (Yb=5 mol %, Er = 5 mol %), Yb/Er ratio of 2.33 (Yb=7 mol %, Er = 3 mol %) thereafter decreases continuously until Yb/Er ratio of 9 (Yb = 9 mol %, Er =1 mol %) the efficiency drop to near 8 ± 1.20 %. The pattern of the downconversion QY as show in Fig. S3 clearly indicates that downconversion QY for 1550 nm emission in Er/Yb :La_2O_2S is maximum for 9 mol% Er^{3+} and minimum for 1% Er^{3+}

The higher downconversion QYs for 1550 nm emission in higher Er^{3+}contained sample is obvious. Being the metastable state Er^{3+} ($^4I_{13/2}$) with the longest lifetime of 2.78 ms and 3.88 ms compared to other levels as reported for La_2O_2S: 1 mol % Er and La_2O_2S: 9 mol %Yb/ 1 mol %Er, measured under pulsed 980 nm excitation; should give the most intense 1550 nm emission. The measured downconversion QY (980 to 1550 nm) pattern with varying Er^{3+} concentration validates our measurement setup. We also compare our downconversion absolute QYs data for La_2O_2S: Yb/ Er with the upconversion QY measured for Gd_2O2S: 10 % Er reported recently by Rodriguez et al.[3] In his work, he has achieved the maximum upconversion QY of 12 ± 1% for Gd_2O_2S: 10 % Er at the excitation power density of 0.07 W/cm^2 under 1550 nm excitation. Reported absolute QY with upconversion (two and three photon) process for Gd_2O_2S: 10 % Er, validates our concentration dependent downconversion (one photon process) QYs setup and data obtained for different concentration of La_2O_2S: Er/Yb. Based on our observations, reproducibility of a given measurements are likely within 2.5 %.

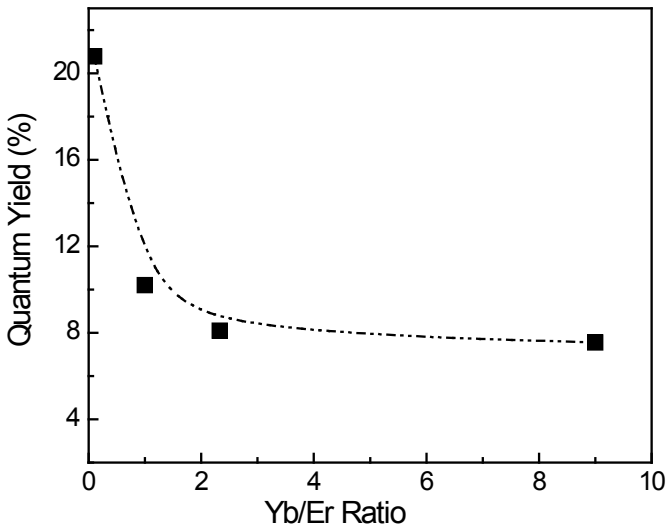

Fig. S3. Downconversion quantum yield in La2O2S: Yb/Er phosphor for the emission at 1550 nm at the excitation power density of 2.4 W/cm2 under 980 nm excitation. The dashed lines are for guiding the eye.

ESI-S4

At the excitation power density 12.74 W/cm2 under 800 nm excitation

Using filter with OD=2.0

Area under Laser profile with Ref (A_L)	Area under Laser profile with sample A'_L(sample)	Area Under the emission spectra (A_e)	$QY=A_e/A_L-A'_L$	QY %
1035*10^2	948.42*10^2	933.37	933.37/8.65*10^3	10.79%
1032*10^2	936.32*10^2	923.25	923.25/9.568*10^2	9.6%

Average QY=10.2 ± 1.53 %

At 5.3 W/cm^2, using filter with OD=2.0

Area under Laser profile with Ref (A_L)	Area under Laser profile with sample A'_L(sample)	Area Under the emission spectra (A_e)	$QY=A_e/A_L-A'_L$	QY %
741.48*10^2	639.58*10^2	508.78	508.78/1.02*10^4	5.00 %
748*10^2	644*10^2	524.10	524.10/1.04*10^2	5.04 %

Average QY=5.02 ± 0.75 %

Since the laser was causing the detector to saturate, neutral density filters with optical density OD=2.0 was used to avoid the saturation on detector, later area under laser with reference and sample were multiplied by 10^2.

Different approach for the Calibration of Integrating Sphere

ESI-S5 Comparison Approach for downconversion (Stokes emission) QY measurement for powder Nd^{3+}:GdF_3

In order to calibrate the integrating sphere and IR detector, we first measured the QY for dye (IR 140) under 800 nm excitation. With the known quantum yield of 10 % for IR-140 dye at the spectral range of 862-1013 nm range at 150 mW of excitation power under 800 nm excitation, relative approach was first implemented for the measurement. Relative measurement for 1% Nd^{3+}:GdF_3 solid powder shows the downconversion QY for 1% Nd^{3+} :GdF_3 is 5.8 ± 0.87 % at 150 mW of excitation under 800 nm as shown in Fig.S5. The beam size of the excitation beam was 1 mm. With the beam size of 1 mm, the calculated power density comes to be 4.77 W/cm^2. With this excitation power density, we then calculated the downconversion QY for 1% Nd^{3+}: GdF_3 using integrating sphere setup. In the integrating sphere setup, we measured the QY for 1% Nd^{3+} :GdF_3 to be 5.02 ± 0.75 %. This clearly validates and calibrates our measurement setup with integrating sphere.

For the relative measurement, area under the spectrum was used to evaluate the quantum yield for 1% Nd^{3+}:GdF_3.

$$\frac{A_1}{A_2} = \frac{\eta_1}{\eta_2} \Rightarrow \frac{70}{119} * 10\% = 5.8\%$$

Where A_1, and A_2 represents the area under the emission spectra for the IR-140 at 4.77 W/cm^2 and 1% Nd^{3+}:GdF_3 under 800 nm excitation as shown in Fig.S5. Similarly η_1 represent the known QY for IR-140 and η_2 represents the unknown QY for 1% Nd^{3+}:GdF_3 at the excitation power of 150 mW under 800 nm excitation.

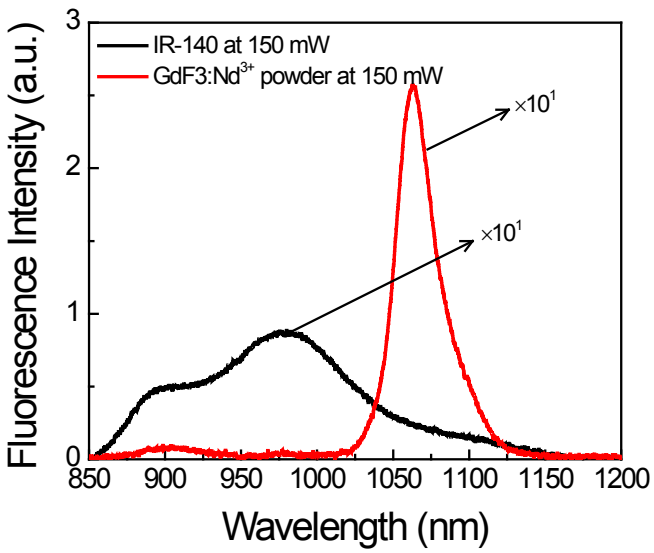

Fig. S5. Fluorescence spectra for the IR-140 and for GdF_3:1% Nd^{3+} collected under the identical condition for the calculation of QY using comparison method. Neutral density filter with optical density O.D.=1.0 was used to avoid the detector saturation.

ESI-S6 Dispersion stability of GdF_3: 1% Nd^{3+} nanoparticles

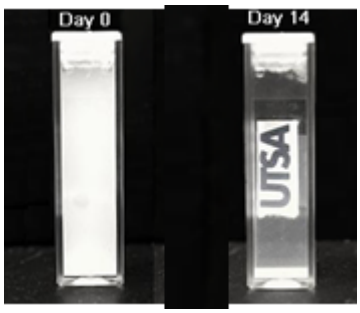

Fig. S6 Dispersion stability of GdF_3: 1% Nd^{3+} nanoparticles in deionized water. Even after two week we still can see that the water still has particles in suspension

ESI-S7 Quantum Yield for Colloidal GdF_3:Nd^{3+}

Relative method was implemented to measure the downconversion QY for colloidal GdF_3:1% Nd^{3+} with respect to reported QY for the dye IR-140 under the identical environment.[4] The measurements for colloidal GdF_3:1% Nd^{3+} were mimicked based on the reported literature for IR-140.[4] Using the QY of 10 % reported for the IR-140 at 150 mW (4.77 W/cm^2) of excitation under 800 nm, downconversion QY for GdF_3:1% Nd^{3+} at the concentration of 0.05 mg/mL was measured to be 1 ± 0.05 %. For later measurements with high power density, the first measured value of QY for GdF_3:1% Nd^{3+} was used as a standard. QY of 1.5 ± 0.075 % was measured for GdF_3:1% Nd^{3+} at 255 mW (8.28 W/cm^2). The spectra collected for colloidal GdF_3:1% Nd^{3+} at different powers is shown in Fig. S7 with respect to the spectra for IR-140 at 800 nm excitation. Moreover, QY for colloidal GdF_3:1% Nd^{3+} was found concentration and excitation power dependent.

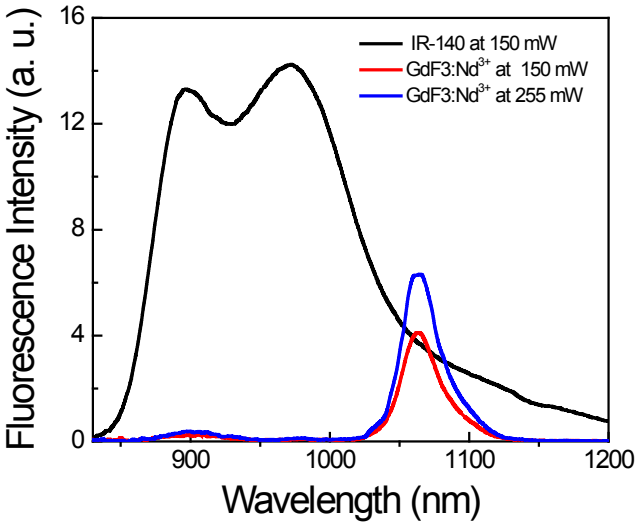

Fig.S7. Fluorescence spectra for the IR-140 and for colloidal GdF_3:1% Nd^{3+} collected under the identical condition for the calculation of QY using comparison method.

ESI-S8. pH Independent Fluorescence Properties for GdF_3: 1% Nd^{3+}

For many applications in biological media, it was essential that a biomarker have pH independent fluorescence QY. Therefore, a pH dependence fluorescence QY study was conducted using deionized water (pH 7.0), HCl 0.1M solution (pH 2.0), NaOH 0.1M solution (pH 10.0), and Minimum Essential Media (MEM) Alpha with 10% Fetal Bovine Serum (pH 7.4) at a GdF_3; Nd^{3+} (1.0%) concentration of 40 mg mL^{-1}.

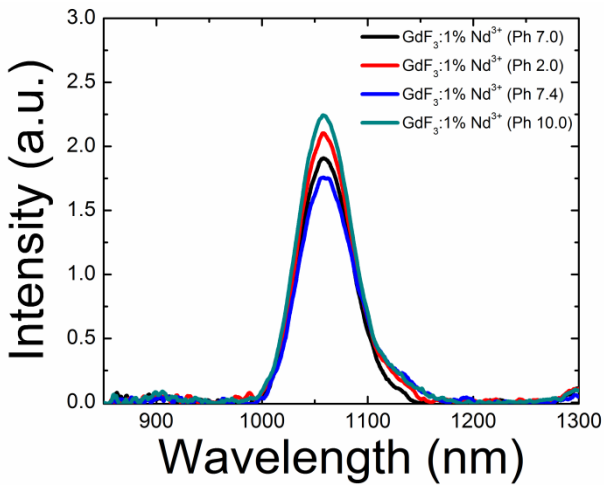

Fig. S8. The emission profile of GdF_3: 1% Nd^{3+} nanoparticles at a concentration of 40 mg mL^{-1} with: deionized water (pH 7.0), HCl 0.1M solution (pH 2.0), NaOH 0.1M solution (pH 10.0), and Minimum

Essential Media (MEM) Alpha with 10% Fetal Bovine Serum (pH 7.4).

ESI. S9. Confocal Imaging

Fibroblast cells (L929) were seeded and grown on glass cover slips. The nanophosphors were infused into growth media by vigorous vortexing at a concentration of 200 μgmL^{-1}, and the cells were incubated in it for 24 hours. Finally, the cells were washed three times with PBS to remove excess nanophosphors. Then the nuclei was stained with DAPI, and the cytoplasm with Alexa Fluor 647 phalloidin. The samples were then fixed and mounted on microscope slides for imaging.

ESI. S10. Absorption Cross- section for 1% Nd: GdF_3 at room temperature

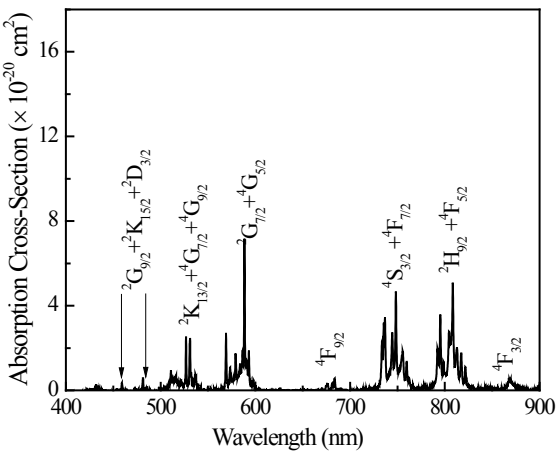

Fig. S9. Absorption cross-section spectrum of 1% Nd^{3+}: GdF_3 nanocrystals at room temperature ranging between 300 and 1000 nm.

ESI. S11. Absorption and Emission cross-section for 1% Nd^{3+}: GdF_3 nanocrystals and absorption coefficient of water at room temperature

Parameters	1% Nd^{3+}: GdF_3
Absorption Cross-section for 1% Nd^{3+}: GdF_3 (σ_a cm^2) at 488 nm	$0.09 \acute{} 10^{-20}$
Absorption Cross-section for1% Nd^{3+}: GdF_3 (σ_a cm^2) at 800 nm	$5.06\acute{} 10^{-20}$
Emission Cross-section for 1% Nd^{3+}: GdF_3 (σ_e cm^2) at 532 nm under 488 nm excitation	$0.08\acute{} 10^{-20}$
Emission Cross-section for 1% Nd^{3+}: GdF_3 (σ_e cm^2) at 1064 nm under 800 nm excitation	$3.91\acute{} 10^{-19}$
Water absorption Cross-section (σ_a cm^2) at 1064 nm	$0.13\acute{} 10^{-20}$
Water absorption coefficient (cm^{-1}) at 1064 nm[5]	0.25
Water absorption coefficient (cm^{-1}) at 532 nm	0.00447

Spectral analysis shows that these particles possesses fifty six times higher absorption cross section at 800 nm excitation compared to that of 488 nm excitation and four hundred and eighty times higher emission cross-section at the emitting wavelengths (1064 nm) under 800 nm excitation compared to that of 532 nm emission under 488 nm excitation. These results are consistent with the previously published results for Nd:YAG nanoparticles.[6] Water absorption cross-section data have been taken from the literature.[7]

Notes and references

1. M. Pokhrel, A. k. Gangadharan and D. K. Sardar, *Materials Letters*, 2013, **99**, 86-89.
2. M. Pokhrel, G. A. Kumar and D. K. Sardar, *Journal of Materials Chemistry A*, 2013.
3. R. Martín-Rodríguez, S. Fischer, A. Ivaturi, B. Froehlich, K. W. Krämer, J. C. Goldschmidt, B. S. Richards and A. Meijerink, *Chemistry of Materials*, 2013.
4. M. Leduc and C. Weisbuch, *Optics Communications*, 1978, **26**, 78-80.
5. C.-L. Tsai, J.-C. Chen and W.-J. Wang, *Journal of Medical and Biological Engineering*, 2001, **21**, 7-14.
6. M. Pokhrel, N. Ray, G. A. Kumar and D. K. Sardar, *Opt. Mater. Express*, 2012, **2**, 235-249.
7. J. A. Curcio and C. C. Petty, *J. Opt. Soc. Am.*, 1951, **41**, 302-302.

AUTHOR INFORMATION

Corresponding Author

*Madhab Pokhrel
Department of Physics and Astronomy
University of Texas at San Antonio
One UTSA Cirlce, San Antonio, Texas 78249, United States
(*) E-mail: ekf012@my.utsa.edu

Author Contributions

*Madhab Pokhrel, L.C. Mimun, Gangadharan Ajithkumar, Brian Yust, and Dhiraj K Sardar,
Department of Physics and Astronomy
University of Texas at San Antonio
One UTSA Cirlce, San Antonio, Texas 78249, United States
(*) E-mail: ekf012@my.utsa.edu

Ashish Dhanale, Liang Tang
Department of Biomedical Engineering University of Texas at San Antonio One UTSA Circle,
San Antonio, Texas 78249